



Comparative Study of Stress Intensity Factor of Some Engineering Materials

John U. Arikpo*, Michael U. Onuu and Brian E. Usibe
Department of Physics, University of Calabar, Calabar-Nigeria.

ARTICLE INFO

Article history:

Received: 14 October 2013;

Received in revised form:

10 December 2013;

Accepted: 20 December 2013;

Keywords

Stress intensity factor,
Modes of fracture,
Crack-tip element size,
Engineering materials.

ABSTRACT

Comparative study of stress intensity factor (SIF) for modes I, II and III were investigated for some engineering materials. The materials are alumina, iron, mild steel, low carbon steel, stainless steel, concrete, silica glass and PVC. Special crack-tip element method was implemented to evaluate the stress intensity factor (SIF) for centre, single-edge and double-edge crack for various values of shear modulus and symmetric crack-tip element size. Different SIF for various modes were compared for these materials and the results from the plots show that low carbon steel for mode III and alumina for mode II have high resistance to crack-growth at $12.43 \text{ MPa}\sqrt{m}$ and $12.2 \text{ MPa}\sqrt{m}$ SIF, respectively between the bounds of shear modulus 1.39 and 2.23. Also alumina for mode I exhibited crack growth at $1.42 \text{ MPa}\sqrt{m}$ SIF and 1.15 bounds of shear modulus. Mode I for mild steel, iron and stainless steel exhibited crack-growth at $0.691 \text{ MPa}\sqrt{m}$ SIF and 1.08 bounds of shear modulus. Mode I is anomalous to crack-tip element size while modes II and III show exponential decay but with crack growth in concrete and abscissa to the coordinate of PVC.

© 2013 Elixir All rights reserved

Introduction

Through the ages, the application of materials in engineering design has posed difficult problems to mankind. Experience has shown that structures built of these materials did not always behave satisfactorily and unexpected failures often occurred. Material failures occurred under conditions of low stresses which made them apparently mysterious flaws and stress concentrations.

The main objective of this comparative study is to predict material behaviour at the application of stress. Many methods could be used in the study of structural behaviour of engineering materials. Well (1971) has demonstrated that crack opening displacement (COD) approach is concise at low stress or above and beyond general yield point. The knowledge of plane stress fracture mechanics of steel is of paramount importance in understanding the behaviour of thin structures containing steel with crack-like flaws or other stress raiser (Onuu and Adjepong, 1994).

The stress intensity factor "K" is used in fracture mechanics to predict the stress state near the tip of a crack caused by a remote load or residual stresses (Anderson, 1995). It is a theoretical concept usually applied to a homogenous linear elastic material and is used for providing a failure criterion for brittle materials. The magnitude of "K" depends on sample geometry, the size and location of the crack and magnitude and the modal distribution of loads on the materials. Different subscriptions are used to designate the stress intensity factor for the three different fracture modes. The quarter point traction and the displacement crack tip elements were adopted by Tan and Gao (1992), who used analytical expressions for the stress intensity factor given by the nodal traction and displacement of these elements. Synder and Cruse (1975) used the single crack Green's function to calculate the stress intensity factors analytically without modelling the crack surface.

The materials used in this investigation of stress intensity factor for modes I, II and III are: alumina, iron steel, low carbon steel, mild steel, stainless steel, silica glass, concrete and polyvinylchloride (PVC).

Elastic moduli

The elastic moduli for two-dimensional (2-D) homogenous body which is isotropic is first considered for such materials; the relationship between the stress tensor σ_{ij} and strain tensor ϵ_{ij} is given by

$$\sigma_{ij} = (K - G)\epsilon_{kk}\delta_{ij} + 2G\epsilon_{ij} \quad i, j, k = 1, 2 \quad (1)$$

Equation (1) defines the 2-D bulk modulus K , and shear modulus G . Note that the symmetric stress and strain tensors have three independent components. Similarly, we write the strain-stress relation as

$$\varepsilon_{ij} = \frac{1}{E} [(1+\nu)\sigma_{ij} - \nu\sigma_{kk}\delta_{ij}], \quad i, j, k = 1, 2 \quad (2)$$

where ν and E are the 2-D Poisson's ratio and Young's modulus, respectively. Clearly there are only two independent moduli. Comparing equations (1) and (2) yields e.g., the following interrelations:

$$G = \frac{E}{2(1+\nu)} \quad (3)$$

$$\nu = \frac{K-G}{K+G} \quad (4)$$

An asymptotic relation for the materials was obtained in an incompressible matrix near the close packing volume fraction. Specifically, we find that the critical component is 34 in contrast to component $-1/5$ appearing in relation.

Recently, Thorpe and Jasiuk (unpublished) have noted that both Poisson's ratio and Young's modulus obey the law of mixtures. The boundary element method (BEM) used provides a very efficient way to compute effective elastic properties of composite materials. Becker (1992) provides a comprehensive treatment of the numerical solution of the BE equation including treatment of inclusions.

Table 1.1: Some materials constants (Ashby and Jones,1980).

Materials	Young's modulus E/GNm^{-2}	Poisson Ratio ν	Expansion coefficient $K^{-1} \times 10^{-6}$	Fracture toughness $MNm^{\frac{1}{2}}$
Alumina	390	0.25	7.0	3-5
Iron	190	0.30	13.0	150
Low alloy steel	200-210	0.30	15.0	50
Stainless steel	190-200	0.30	11.0	30
Mild steel	196	0.30	15.0	140
Silica glass	94	0.16	0.50	0.0008-0.0048
Aluminium & alloys	69-79	0.35	2.20	20-50
Concrete (reinforced)	45-50	0.3	10.0	10-15
PVC	0.003-0.01	0.41	70.0	2.0-4.7

Crack-tip element method

Crack-tip element method is the type of boundary element method used by Wu (2004) to evaluate the stress intensity factors for modes I, II and III respectively such as

$$K_I = B_y \frac{G}{k+1} \sqrt{2\pi} \quad (5)$$

$$K_{II} = B_x \frac{G}{k+1} \sqrt{2\pi} \quad (6)$$

$$K_{III} = B_z \frac{G}{4} \sqrt{2\pi} \quad (7)$$

where G is the Shear modulus, ν is the Poisson's ratio, $k = 3 - 4\nu$ for plane strain (very thick materials)

B_y = geometric correction factor for Centre Crack (CC)

B_x = geometric correction factor for Single-edge Crack (SEC)

B_z = geometric correction factor for Double-edge Crack (DEC)

where $(\frac{a}{W})$ = crack size (specimen geometry), a =crack length, w =crack width.

Crack configurations and related geometric correction factors for compliance constants was used to calculate the stress intensity factor for the different modes. The compliance constants are;

$$B_y = \left[1 + 0.50\left(\frac{a}{W}\right)^2 + 20.46\left(\frac{a}{W}\right)^4 + 81.72\left(\frac{a}{W}\right)^6 \right]^{\frac{1}{2}} \tag{8}$$

$$B_x = 1.12 - 0.23\left(\frac{a}{W}\right) + 10.55\left(\frac{a}{W}\right)^2 - 21.71\left(\frac{a}{W}\right)^3 + 30.38\left(\frac{a}{W}\right)^4 \tag{9}$$

$$B_z = 1.12 + 0.41\left(\frac{a}{W}\right) - 4.78\left(\frac{a}{W}\right)^2 + 15.44\left(\frac{a}{W}\right)^3 \tag{10}$$

Below is the crack tip elements (C) at the different boundaries for materials with centre-and single-edge crack.

Figure (1) shows typical crack element meshes for a centre crack of length $2a$, where C is the crack tip element size and figure (2) shows the crack element meshes for an edge crack.

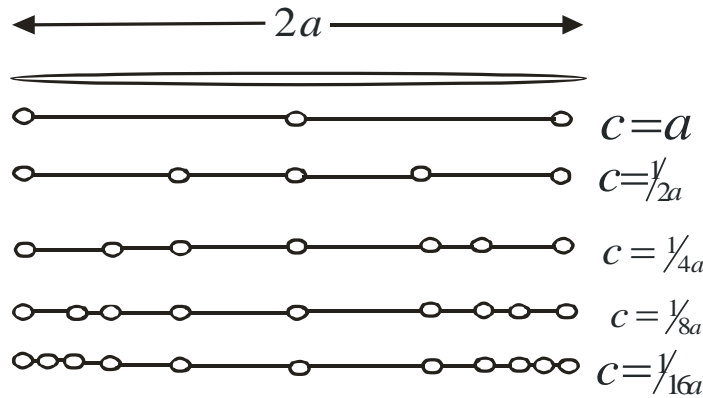


Fig. 1: Symmetric crack elements for a centre crack

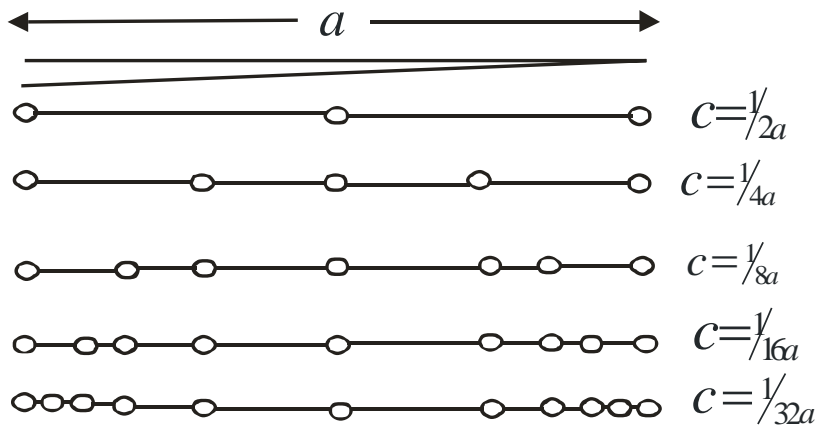


Fig. 2: Symmetric crack elements for a an edge crack

Shear modulus (G) calculation

The two-dimensional (2D) effective shear modulus was calculated by substituting the values for the Elastic Young’s modulus (E) and Poisson’s (ν) ratio obtained from table 1.1: Some material constants (Ashby and Jones, 1980) for the different materials into equations (11)

$$G = \frac{E}{2(1+\nu)} \tag{11}$$

The model developed by Eischen (1993) was used to calculate the upper and lower bounds shear modulus of the materials as shown in equations (12) and (13)

$$G_L^{(3)} = \left[\left\langle \frac{1}{G} \right\rangle - \frac{\phi_1 \phi_2 \left(\frac{1}{G_2} - \frac{1}{G_1} \right)^2}{\left\langle \frac{1}{\tilde{G}} \right\rangle + \langle G \rangle_\eta} \right]^{-1} \quad \text{(lower bound)} \quad (12)$$

$$G_U^{(3)} = \langle G \rangle - \frac{\phi_1 \phi_2 \left(\frac{1}{G_2} - \frac{1}{G_1} \right)^2}{\left\langle \tilde{G} \right\rangle + \langle G \rangle_\eta} \quad \text{(upper bound)} \quad (13)$$

where $G_U^{(3)}$ = upper bound shear modulus

$G_L^{(3)}$ = lower bound shear modulus

\tilde{G} = average shear modulus

G_2 = highest value of the shear modulus

G_1 = lowest value of the shear modulus

G = shear modulus for alumina, iron steel, low carbon steel, mild steel, stainless steel, silica glass, concrete or polyvinylchloride (PVC).

ϕ_2 = material volume fraction (set values 0.1- 0.85)

ϕ_1 = material volume fraction

$\langle G \rangle_\eta$ = shear modulus as a function of the microstructural parameter

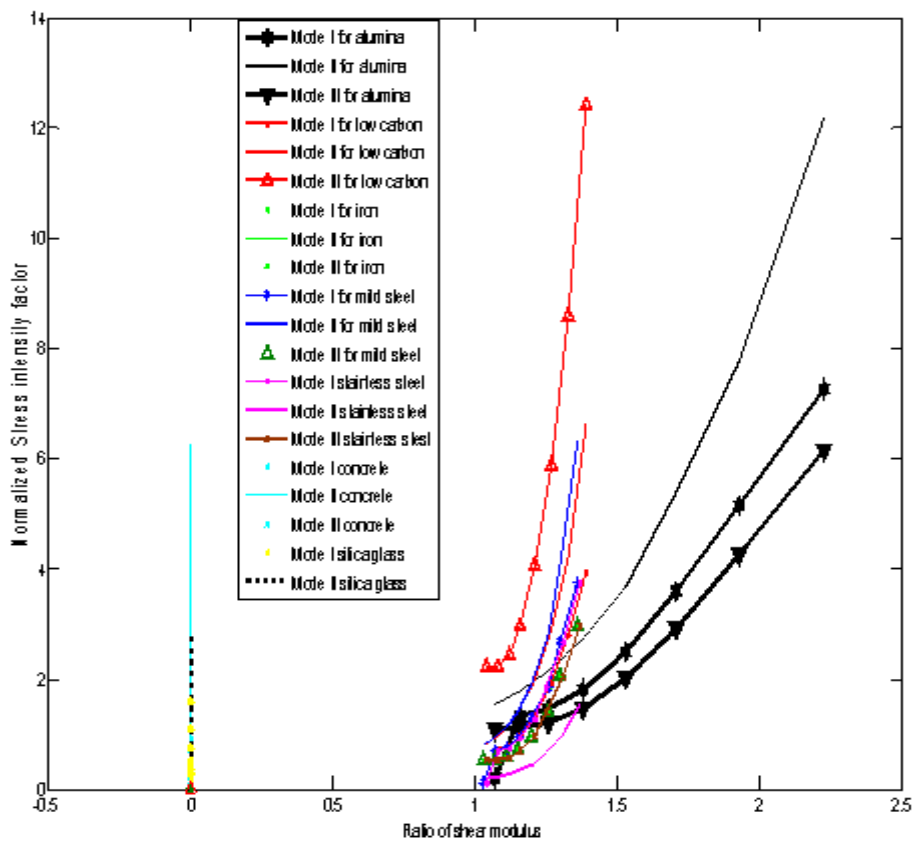


Fig. 3: Stress intensity factor vs. ratio of shear modulus for the materials

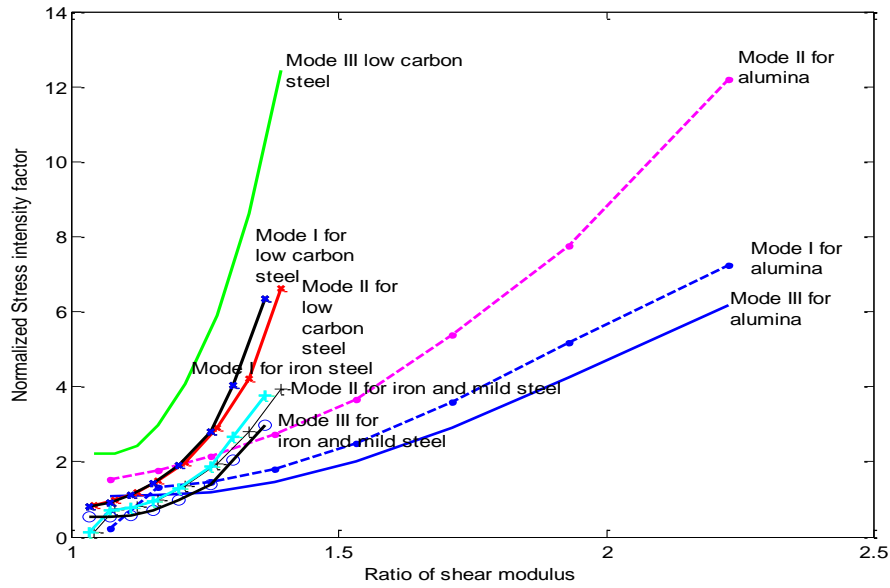


Fig. 4: Plot of Stress intensity factor for different materials

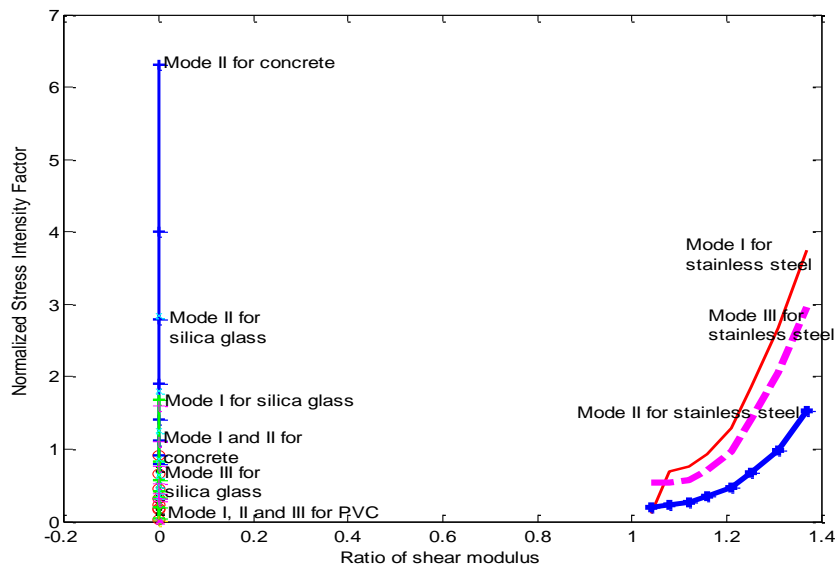


Fig. 5: Stress intensity factor for different modes in ceramics

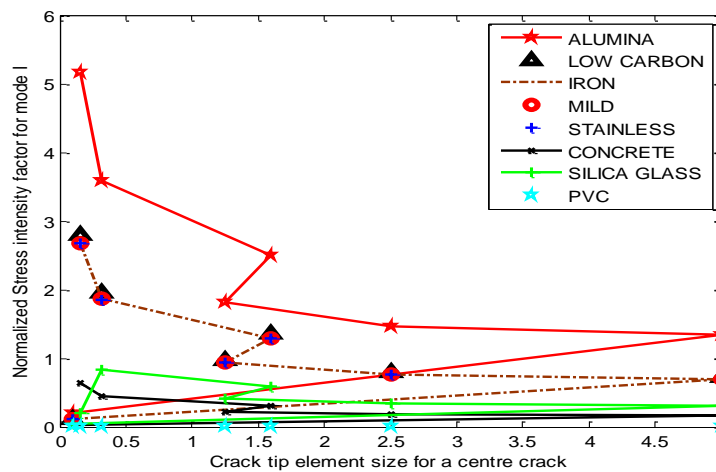


Fig. 6: Effect of stress intensity factor on symmetric crack tip element for mode I

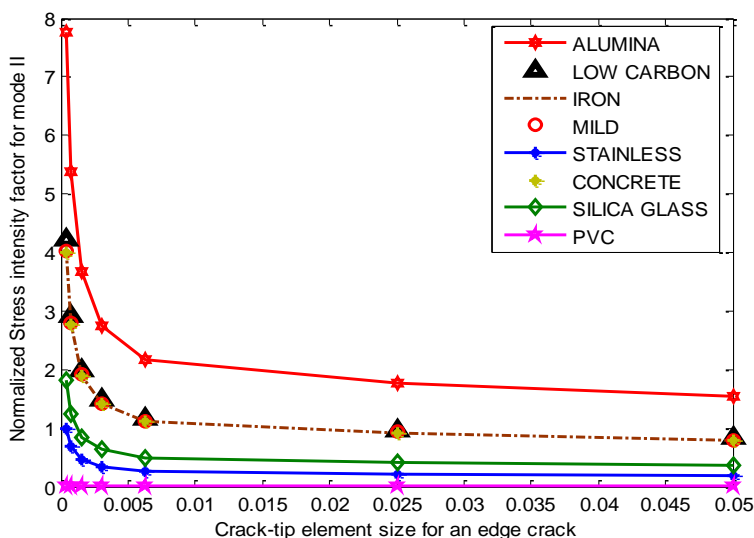


Fig. 7: The effect of stress intensity factor on symmetric crack tip element for mode II

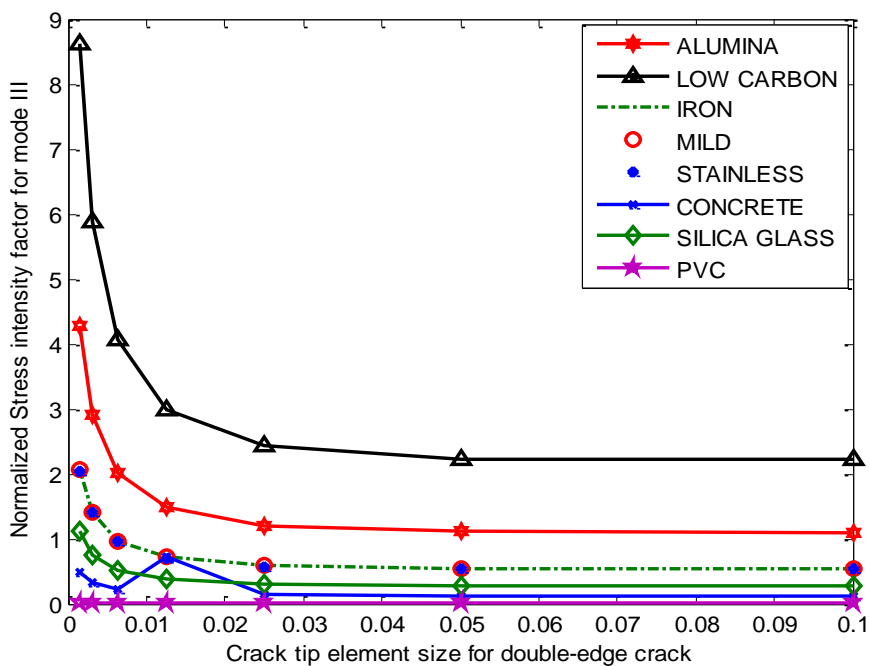


Fig 8: The effect of stress intensity factor on symmetric crack tip element for mode III

Results and discussion

Figure 3 shows a plot of family of stress intensity factor curves for modes I, II and III respectively at the different ratio of shear modulus for metals and ceramics. All the curves responded differently in a peculiar way, in this plots low carbon steel for mode III and alumina for mode II has high resistance to crack growth at $12.43 \text{ MPa} \sqrt{m}$ and $12.2 \text{ MPa} \sqrt{m}$ stress intensity factor between the bounds of shear modulus 1.39 and 2.23.

The stress intensity factor for alumina in mode II loading is higher than mode I and mode III loading, this shows that alumina for mode II is more resistive to crack growth. While mode I for same material exhibited crack growth at $1.42 \text{ MPa} \sqrt{m}$ stress intensity factor and 1.15 bounds of shear modulus.

Low carbon steel for mode III loading is more resistive to crack growth than mode II and mode I.

Mode II loading for iron and mild steel is higher than mode I and mode III. Mode I for mild steel, iron and stainless steel exhibit crack growth at $0.691 \text{ MPa} \sqrt{m}$ stress intensity and 1.08 bounds of shear modulus.

Modes I, II and III for the following materials: silica glass, concrete and PVC are extrapolated into a vertical plot.

Figure 4 shows stress intensity factor curves for different modes in metals, the curves show exponential increase in response as the ratio of shear modulus increases this is in agreement with Eischen and Torquato (1993), particularly low carbon steel for mode III and alumina for II appear to have the highest stress value while mode II, III for iron and mild steel has the lowest stress intensity factor with crack initiation at $0.69 \text{ MPa} \sqrt{m}$

Figure 5 shows the plot of stress intensity factor for different modes in ceramics. Modes I, II and III for concrete, silica glass, and PVC responded vertically to stress intensity factor at 0 ratio of shear modulus while mode I, II and III for stainless steel rises from 1.02 shear modulus. Figure 6 shows that stress intensity factor for mode II loading decay exponentially asymptotic to the crack-tip element size and alumina exhibited the lowest decay while stainless steel exhibited the highest decay. Similar results were obtained in fracture characterization of ST60Mn by J-Integral method (Onuu, 2000). Plots (Figure 7) for mode II and (Figure 8) for mode III decay exponentially with crack growth in concrete and abscissa to the coordinate of PVC.

Conclusions

The essence of material analysis is to investigate the mode of fracture loading that can initiate crack growth in engineering materials used for design and construction. From the comparisons of stress intensity factor for different modes it could be concluded that crack growth is predominant in mode I loading for alumina, mild steel, iron and stainless steel

Modes I, II and III for the following materials silica glass, concrete and PVC are extrapolated into a vertical plot at zero showing infinite response. While low carbon steel for mode III and alumina for mode II has high resistance to crack growth. The anomalous behaviour of mode I stress intensity factor to crack tip element size is due to the fact that the displacements are symmetric with respect to the x-z and x-y planes.

References

- A. A. Becker (1992). *The boundary element method in Engineering* McGraw-Hill, New York.
- Anderson, T. L. (1995). *Fracture Mechanics: Fundamentals and Applications* CRC press wikipedia.org/wiki/Fracture_mechanics.
- Ashby, M. F. & Jones, D. R. H. (1980). *Engineering Materials I: An Introduction to their Properties and Applications*, Pergamon Press Ltd., 31
- Broek, D. (1986). *Elementary Engineering Fracture Mechanics'*, Fourth edition, Kluwer Academic Publisher, Boston.
- Burdekin, F. M. and Stone, D. E. W (1966). The crack opening displacement approach to fracture mechanics in yielding materials, *journal of strain Analysis* 1 145-153.
- Bower, A. F. (2008). *Applied Mechanics of Solids Engineering Fracture Mechanics* 69, 267-280.
- Eischen, J. W & Torquato S.(1993) *Determining elastic behavior of composites by the boundary element method* Princeton University, new Jersey 08544
- M. F. Thorpe and I. Jasuik (unpublished)
- Onuu, M. U. & Adjepong, S. K. (1994). Investigation of Plane Stress Fracture Mechanics Parameters of Locally Produced Steel. *Nigeria Journal of Physics*, 6, 8-15.
- Onuu, M. U. (2000). The study of fracture characteristics of ST60Mn steel by J-Integral method *JAS* 3,(1) 663- 673
- Onuu, M. U. (2010). *Engineering Material Lecture Notes*, University of Calabar. Nigeria
- Snyder, M. D. & Cruse T. A. (1975). Boundary integration equation analysis of cracked anisotropic plate. *Int. J Fracture* 11:315-28.
- Tan, C. I. & Gao, Y. L. (1992). Boundary element analysis of plane anisotropic bodies with stress concentrations and cracks. *Comput Struct* 20:17-28.
- Wu, Wei-Liang (2004). *Boundary Element Formulations for Fracture Mechanics Problems*, Ph.D Thesis, School of Mathematics and Applied Statistics, University of Wollongong. <http://ro.uow.edu.au/theses/253>
- Wells, A. A. (1971). The Status of COD in Fracture Mechanics. *Canad. Congr. Applied Mech.* 59-77.